Laser Physics, Vol. 15, No. 7, 2005, pp. 987–996.

Laser Spectroscopy with Nanometric Gas Cells: Distance Dependence of Atom–Surface Interaction and Collisions under Confinement

I. Hamdi[1], P. Todorov[1], A. Yarovitski[1], G. Dutier[1], I. Maurin[1], S. Saltiel[1, 2], Y. Li[1, 3], A. Lezama[1, 4], T. Varzhapetyan[5], D. Sarkisyan[5], M.-P. Gorza[1], M. Fichet[1], D. Bloch[1], and M. Ducloy[1, *]

[1] *Laboratoire de Physique des Lasers, UMR 7538 du CNRS et de l'Université Paris13, 99 Av. JB Clément, F-93430 Villetaneuse, France*

[2] *Department of Physics, University of Sofia, Sofia, Bulgaria*

[3] *Department of Physics, Guyuan Normal University, Ningxia, China*

[4] *IFFI, Universita de la Republica, Montevideo, Uruguay*

[5] *Institute for Physical Research, Armenian Academy of Sciences, Ashtarak 2, Armenia*

*e-mail: ducloy@lpl.univ-paris13.fr

Received January 24, 2005

Abstract—The high sensitivity of laser spectroscopy has made possible the exploration of atomic resonances in newly designed "nanometric" gas cells whose local thickness varies from 20 nm to more than 1000 nm. Following the initial observation of the optical analogous of the coherent Dicke microwave narrowing, the newest prospects include the exploration of long-range atom–surface van der Waals interaction with spatial resolution in an unprecedented range of distances, modification of atom dielectric resonant coupling under the influence of the coupling between the two neighboring dielectric media, and even the possible modification of interatomic collision processes under the effect of confinement.

The high sensitivity of laser spectroscopy has recently made possible the exploration of atomic resonances in newly designed "nanometric" gas cells. We discuss here some of the novel features and prospects that arise from these resonant confined gases.

1. OPTICAL SPECTROSCOPY IN MICRO- AND NANOCELLS

For a very dilute gas, it is rather common, although an unfamiliar idea, that the atomic "mean free path" is actually governed by the container geometry. Designing specific vapor cells with parallel windows and a very small thickness enables one to make the mean free path strongly anisotropic, since atoms fly from wall to wall if the vapor is dilute enough. In these conditions, the transient buildup of the resonant interaction with light is responsible for a specific enhancement of the response of the slow (with respect to the normal velocity, i.e., the velocity component along the normal to the windows) atoms. As long as the irradiation is under normal incidence, this provided the principle for a novel method of Doppler-free spectroscopy, applicable to a variety of situations (velocity-dependent optical pumping, linear absorption, two-photon transition, etc.; see [1] and references therein). The initial demonstrations were operated with glass cells of commercial origin, filled with alkali-metal vapors, and whose thickness (10–1000 μm) remained much larger than the optical wavelength λ. Because of that, the amplitude of the specific sub-Doppler signal was limited, and the effects of the atom–surface interaction [2] remained unobservable; currently, however, we can investigate them (see, e.g., [3] and references therein) thanks to developments in selective reflection (SR) spectroscopy, a method known to offer probing for a typical reduced wavelength $\lambda/2\pi \sim 100$ nm.

The recent fabrication of extremely thin cells (ETC) of vapor [4], designed with an initial submicrometric spacer between two carefully polished parallel windows, has revealed that, under the effect of the external atmospheric pressure, the local cell thickness can become extremely small, typically spanning from 20 nm to 1 μm. This truly permits one to investigate so-called nanocells of vapor and has opened a realm of novel prospects that even extends beyond sub-Doppler spectroscopy, with the additional possibility of detecting atom–surface interaction effects in an unexplored range of distances.

The intrinsic accurate parallelism of the windows (e.g., a deviation <1 μm over a 10-mm transverse extension) implies an intrinsic Fabry–Perot behavior. Although it is convenient to evaluate the local thickness of the nanocell through irradiation at nonresonant wavelengths, this behavior tends to unavoidably mix up the elementary behaviors associated with reflection and transmission spectroscopies [5]. Also, it naturally exhibits a λ/2 periodicity.

Aside from this periodic interference effect, the spectral width exhibits complex variations with the nanocell length, as a combined result of the simulta-

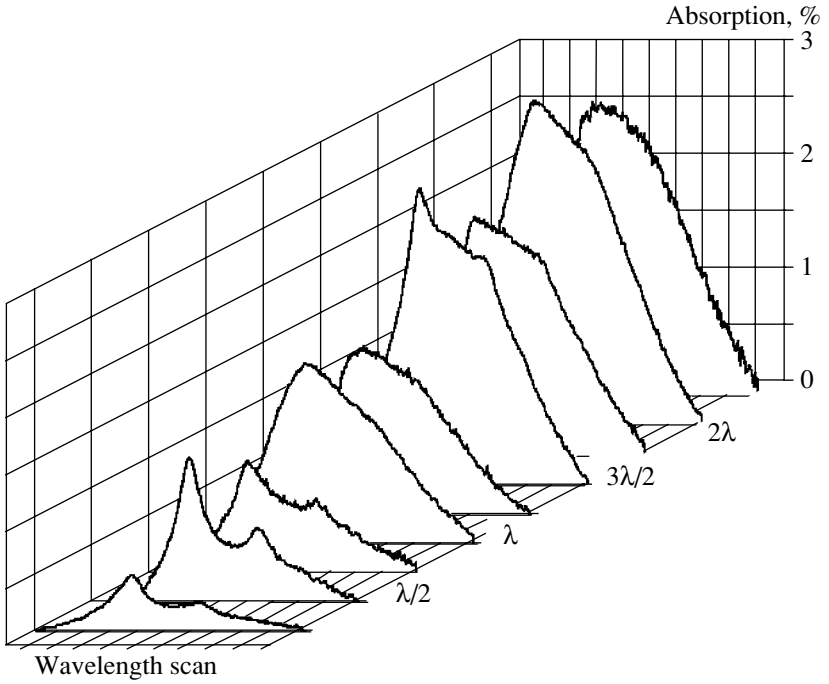

Fig. 1. Experimental transmission line shapes as observed on the ^{87}Rb D_2 line (wavelength scan $F = 2 \longrightarrow F' = 3, 2, 1$) for various nanocell thicknesses (multiples of λ/4) at a nonsaturating power (~0.4 mW/cm^2). The vertical scale has been normalized with respect to the nonresonant Fabry–Perot transmission. The narrow structures appearing for λ/2 and, with a smaller contrast, for 3λ/2, are the signature of the coherent Dicke narrowing.

neous narrowing associated with the contribution from the slow atoms and of the limited interaction time, which implies, finally, a broadening for the smallest thickness. More surprisingly, one also observes a λ pseudoperiodicity in the resonant linear atomic response, with the sharpest spectrum obtained for a λ/2 thickness [6]. Indeed, the linear atomic response features a *coherent* spectroscopic narrowing that extends to the optical domain, in addition to the original observation by Romer and Dicke [7] in the microwave domain of *coherent* spectroscopic narrowing in a gas sample with a thickness ~λ/2. Additionally, a periodical revival of the Dicke narrowing [6, 8] was demonstrated (see Fig. 1). This kind of coherent Dicke narrowing can be viewed as one aspect of the more general consideration, as illustrated by Dicke [9], of the effects of subwavelength confinement in atomic physics, with his related analysis of the Doppler effect in the time domain rather than in the more usual frequency domain.

The coherent spectral narrowing [6–8] relies on the fact that, when an atom leaves the wall, the sudden atom excitation induced by *on-resonance* light starts to precess in phase with the electromagnetic field at the wall position but falls out of phase with the local driving field under the effect of the atomic motion, with the phase mismatch finally reaching kL (L is the cell thickness, k is the wave number). As shown in a Bloch vector model [8], the phase mismatch appearing on the line center under a weak driving field turns to be independent of the atomic velocity because, for wall-to-wall trajectories, it accumulates during a duration L/v at the rate of the Doppler shift kv (v being the normal atomic velocity). Hence, for a cell length up to λ/2 (i.e., a maximal phase shift π), all regions of the cell interfere constructively, whatever the velocity may be, yielding for $L = \lambda/2$ a strong contribution at the line center. In contrast, the signal tends to vanish for $L = \lambda$ as a result of an overall destructive interference between the different regions. For frequency-detuned irradiation, the overall angular precession of the atomic excitation becomes velocity-dependent and leads to a smooth length dependence of the signal that justifies the contrast between the line center and the wings for $L = \lambda/2$. One even observes, for $L = 3\lambda/2$, a revival of the sharp peak at the line center, although its amplitude relative to the background decreases. This oscillating behavior, with a λ (pseudo-) periodicity of the coherent narrowing, fades away for larger values of L, since the atomic dipole relaxation has to be considered when it occurs on a time scale shorter than the time of flight between the walls (i.e., the dipole mean free path becomes small compared to the cell thickness L). The spectral consequences of this behavior are illustrated in Fig. 2.

Fluorescence detection, easily implemented for atomic transitions excited in the visible or near-infrared range [4, 8], also exhibits a strongly sub-Doppler excitation line shape for short cell lengths. However, the

simple picture of a nondegenerate two-level atom, enabling again the use of the Bloch vector model, shows [8] that the fluorescence is essentially insensitive to the interferometric effects that are responsible for the Dicke narrowing. This discrepancy with the linear coherent transmission can be understood in a more general manner from the incoherent nature of the fluorescence process. In addition, the fluorescence, a second-order process, is limited to those atoms slow enough to undergo a successive absorption and emission process. This makes its line shape narrower than the transmission profile even at its narrowest, i.e., for the $L = \lambda/2$ situation.

The linewidth of fluorescence is actually comparable to the one obtained for FM transmission. Indeed, the frequency modulation (FM) version of the nanocell spectroscopy technique is known to be particularly appealing, as for all other *linear* Doppler-broadened systems sensitive to transient effects, such as SR spectroscopy [2, 3]. Since it uses synchronous detection of the optical signal relative to an applied frequency modulation, the FM technique indeed provides the frequency derivative of a direct line shape characterized by a central logarithmic spectral singularity. This singularity, typical of thin-cell spectroscopy, is turned into a pure Doppler-free line shape through the FM technique. In the elementary case of a $\lambda/2$ cell, the usual sub-Doppler linear signal is observed to be narrowed down to a pure Doppler-free signal, while in contrast, the peak amplitude of the measured signal is not reduced, at least as long as the FM amplitude is comparable to the optical width. This makes nanocell transmission spectroscopy one of the very few spectroscopic methods that can be operated in a vapor while being both linear and Doppler-free. It is destined to become an alternate method to saturation spectroscopy for weak, hard-to-saturate transitions, most notably to obtain frequency references from weak molecular transitions that are not suitable for saturated absorption spectroscopy.

Saturation effects in nanocells are also under investigation [10]. The overall trend can be viewed as a survival of the narrow resonances at large intensities, in spite of a washing out of the rapid length dependence (in transmission–reflection experiments) associated with the coherent Dicke narrowing. When optical pumping to an adjacent energy level can occur, the saturation effects, early shown to be velocity-selective and responsible for sub-Doppler features in transmission for a thin cell [11], are incoherent and, like for fluorescence, are insensitive to the coherent Dicke narrowing. This implies that the residual oscillating length dependence experimentally observed upon transmission in *open* two-level systems under strong irradiation should only be traced back to a first-order effect. A systematic study of saturation effects with nanocells shows complex saturation behaviors, including a sharp length dependence that varies with the different hyperfine component under consideration. For the cycling transitions of a degenerate two-level system (i.e., a close two-level system), when the associated coherent behavior is susceptible (in free space) to lead to either a dark absorption line ($J \longrightarrow J' = J - 1$) or a bright absorption ($J \longrightarrow J' = J + 1$), one can observe, over the broad resonant behavior, dips or inverted dips at line center depending on the cell length, in a manner reminiscent of the coherent Dicke narrowing. Theoretically, for these pure two-level systems, the situation is complex because saturation effects remain in the frame of a strong but coherent excitation, so that one may anticipate a residual coherent Dicke effect. However, thin-cell spectroscopy intrinsically explores the dynamics of the atomic response with a velocity distribution that

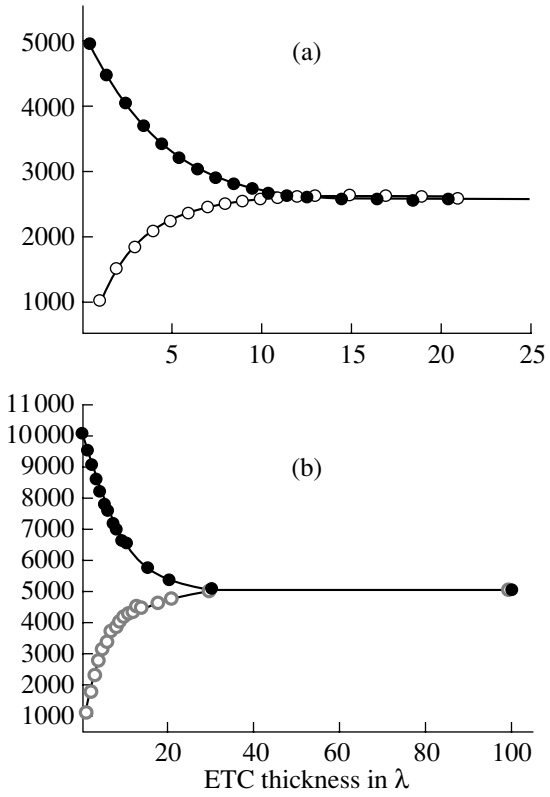

Fig. 2. Calculated peak-to-peak amplitude of the narrow structure in FM transmission as a function of the cell length. The closed circles are for half-integer cell lengths (expressed in number of wavelengths); the open circles are for integer lengths. The decrease in the Dicke revival peaks is exponential with a decoherence length l_c proportional to the dipole mean free path, $l_c \sim 1.15u/\gamma$ (γ is the optical relaxation; u is the thermal velocity). Due to the Doppler-broadened part of the signal that grows monotonically with the cell length and that is not included here, the contrast between the Dicke revival peak and the total signal decreases even faster. The asymptotic nonzero limit corresponds to our initial observation of the Dicke narrowing in a microcell [1]. The Doppler to homogeneous width ratio is given by $ku/\gamma = 25$ (a) or by $ku/\gamma = 50$ (b). In the Doppler limit $ku/\gamma \longrightarrow \infty$, no narrow structure is found at $L = n\lambda$, yielding a zero amplitude for the FM signal (signal derivative).

scrambles this dynamics by the mixing of various time scales, owing to the different Rabi frequencies involved with the Zeeman substates. This complexity of the time sequence of the nonlinear process at least hinders any recognizable Dicke-type pseudoperiodicity.

2. EXPLORING THE ATOM–SURFACE VAN DER WAALS INTERACTION AT SMALL DISTANCES

As mentioned in Section 1, the local thickness of the cell can be monitored through careful interference measurements (e.g., in reflection) operated at various nonresonant wavelengths. On the Cs resonance line (e.g., the D_1 line, $\lambda = 894$ nm), no notable deviations were observed relative to the predictions for a standard isolated two-level atom down to a $\lambda/4$ thickness [6]: the variations of the spectral line shapes with the cell length—in transmission and in reflection as well—simply result from the coherent narrowing in combination with the Fabry–Perot interferences. Indeed, the long-range atom–surface interaction is dominated by the universal van der Waals (vW) attraction $V(z) = -C_3 z^{-3}$ (z is the atom–surface distance) between a fluctuating atom dipole and its image. This attractive potential, whose strength grows with atomic excitation, induces a spectral red shift on the D_1 transition ~1.2 MHz @ 100 nm (for an interaction with a single YAG wall) that is too small to be observed in nanocell spectroscopy for a relatively large thickness. With respect to the Doppler width (~250 MHz) and to the natural transition width (~5 MHz), the onset of a practical observation of the vW interaction appears only for a cell thickness below 200 nm; i.e., all atoms are at a distance from the wall shorter than 100 nm.

The major interest in these nanocells for the probing of the vW interaction is that it extends the possibility of probing short-lived excited states, typical of optical methods such as SR spectroscopy, to an unusual range of short distances. This range can normally be arbitrarily chosen through the choice of the container thickness instead of being imposed by the wavelength of observation, as is the case in SR spectroscopy, with a probe depth $\sim\lambda/2\pi$. This interest is enhanced by the fact that the choice of methods to investigate the long-range atom–surface interaction is actually sparse, in spite of the ubiquity of the vW interaction. Most often, these methods rely on mechanical effects—even for laser-cooled atoms—and are applicable only to ground-state atoms or long-lived states. This explains why the only accurate measurements of the distance law of the interaction have been limited to the 500–3000 nm range (with Rydberg atoms that are strongly interacting and long-lived, allowing for a detection that is partly mechanical) [12]. With nanocells, one envisions the possibility of probing distances at least an order of magnitude smaller, reaching a distance range where limitations to the z^{-3} scaling could originate in various short range effects that have not always been precisely investigated, such as the details in the cell roughness or interaction with impurities sticking to the surface. This z^{-3} scaling normally applies in a typical 1–1000 nm range [2], i.e., as long as retardation (Casimir) effects are negligible and before the occurrence of the short-range effects unavoidably related to a dependence on the atomic structural details of the surface. It thus implies validity over a huge energy range that is particularly worthwhile to test.

Various types of experiments on nanocells have evidenced the effect of the atom–surface interaction. From our most recent analyses, we now expect to be able to shift from the simple observation [13] of the surface interaction to its effective measurement. In particular, it would be very interesting to evaluate the possible accuracy of a vW measurement in nanocell spectroscopy, with respect to that provided by the well-known SR spectroscopy.

Our first step was to analyze the transmission behavior in nanocells on the Cs D_1 resonance line. When the local cell thickness turns to be very small (~50–100 nm), we observe a line shape distortion and a red shift (up to 200 MHz) that largely exceeds those observed through SR spectroscopy. Moreover, the spectral line shapes appear in good agreement with a theoretical model that assumes a known strength of the van der Waals (vW) interaction. This theory simply assumes a thermal distribution of atoms flying from wall to wall and integrates the transient atomic response while taking into account a vW potential. The vW potential itself is modeled according to an electrostatic description that includes the interaction with the multiple images induced in the two reflecting walls. These transmission experiments have been extended to experiments in the FM mode, whose improved spectral resolution is of particular interest for large thicknesses (i.e., when the vW shift remains small), and to reflection spectra: for the smallest thicknesses, reflection spectra are recorded over a low level of nonresonant reflection due to FP interferences and offer a competitive possibility to observe the vW shift [13]. More recently, and as discussed in more detail in Section 4, attempts to fit the recorded spectra with adjustable theoretical curves reveals that taking into account the vW interaction slightly improves the fitting for a 223-nm ($\sim\lambda/4$) thickness (see Fig. 3), while no improvement appears for a $\lambda/2$ thickness.

We are also investigating the stronger vW shift induced in high-lying excited states, such as Cs($6D$), which is probed at 917 nm ($6D_{5/2}$) or 921 nm ($6D_{3/2}$) after a prior excitation on the Cs D_2 line $6S_{1/2} \longrightarrow 6P_{3/2}$ at 852 nm (see Fig. 4). For these 917-nm and 921-nm transitions, the vW interaction should be about an order of magnitude larger than for the D_1 line, at least in the absence of a resonant coupling between the atom excitation and a surface mode. Thanks to a laser diode specially designed for a broad-range tuneability (through

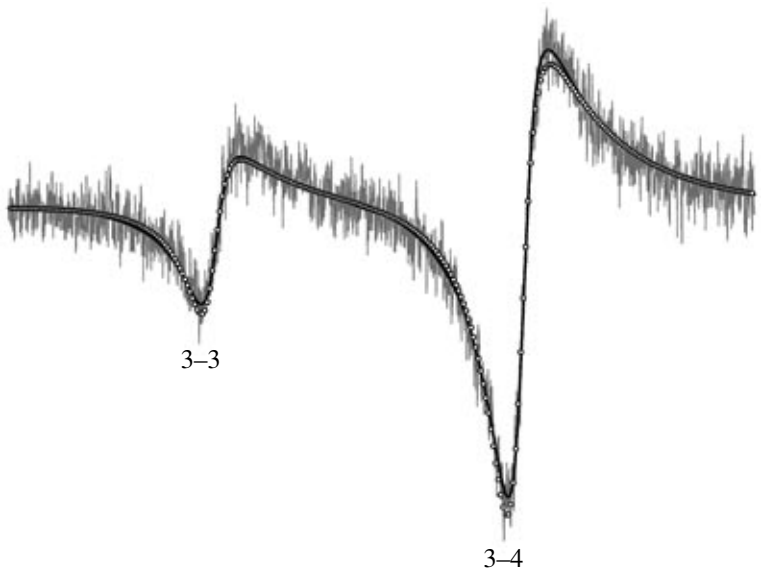

Fig. 3. Reflection spectrum for the Cs D_1 line ($F = 3 \longrightarrow F' = 3, 4$) for a 223-nm ($\lambda/4$) thickness. The experimental data (grey) is fitted with a theoretical line shape taking into account the vW attraction (solid black line) between the two walls or with a less satisfying model that neglects the vW interaction (white dots). The fit here is adjusted for a vW interaction governed by a coefficient ~1.8 kHz μm^3 for a single YAG wall.

step by step frequency changes), we could observe the broadened transmission (and reflection) spectra for various thicknesses down to 20 nm. Depending on the thickness, the observed (red) shift greatly exceeds 10 GHz—i.e., an energy shift about two orders of magnitude larger than those previously observed [12]—while the apparent width of the greatly distorted line shape simultaneously increases with the decrease of the cell length and remains an approximately constant fraction of the frequency shift (i.e., vW-induced inhomogeneous broadening). A preliminary plot (see Fig. 5) of the apparent shift—as measured by evaluating the frequency of the transmission peak—as a function of the local thickness L shows an approximate L^{-3} dependence, an expectation that should be in rough agreement with rigorous theoretical modeling (for a constant relative position z/L, the shift predicted by the theory indeed evolves with L^{-3}, but the apparent shift of the overall line shape is more difficult to evaluate). However, these results can be affected by the pumping process into the intermediate states, including spatial inhomogeneities of the pumping through absorption, possible induced saturation, or dynamic Stark effects, or by the high pressure required for these experiments, which implies broadening and shift.

For this reason, we have turned to a series of systematic experiments for a limited number of cell thickness (presently in the range 40–130 nm) with investigation of the pressure effects and control of the effects of the pumping light. When the experimental conditions ensure that the pump absorption remains weak, with the line shapes remaining independent of the pumping power, the pumping in the $6P_{3/2}$ state can be expected to be nearly thermal.

Hence, it appears reasonable, as was demonstrated in the case of SR spectroscopy on another fine-structure

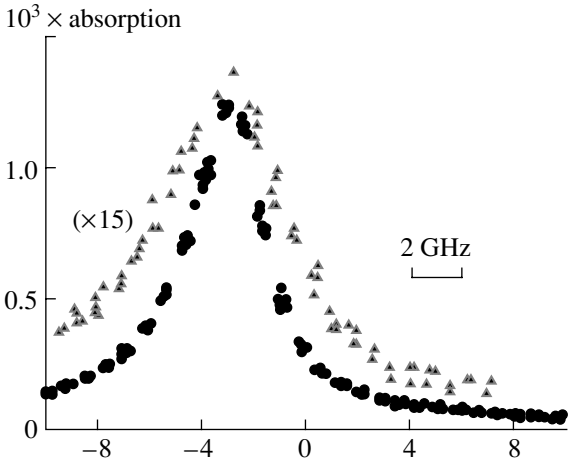

Fig. 4. A comparison between the transmission spectra observed, respectively, on the $6P_{3/2}$–$6D_{5/2}$ (917 nm, black points) and $6P_{3/2}$–$6D_{3/2}$ (921 nm, grey triangles) transitions in a 50-nm-thick Cs cell. The horizontal axis indicates the respective detuning relative to the free-space resonances; the vertical one is the relative (negative) change in transmission. The pumping on the D_2 line induces here only negligible effects, and the results, shown here at $T = 240°C$ (Cs density ~5×10^{15} cm^{-3}) are unchanged for a lower Cs pressure. The spectra here are discontinuous because the laser frequency tuning is only a coarse one, measured with an accuracy close to 100 MHz.

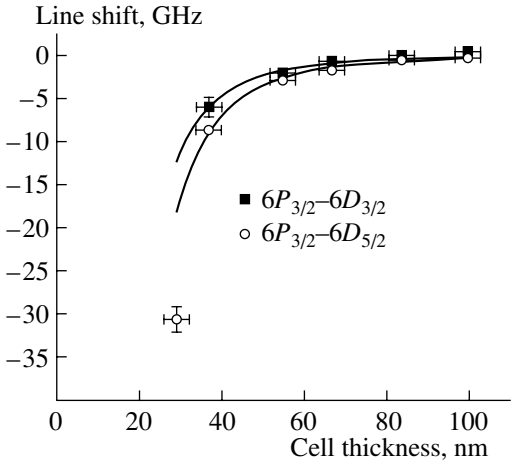

Fig. 5. A preliminary plot of the apparent frequency shift between the transmission peak and the free-space resonances on the $6P_{3/2}$–$6D_{5/2}$ line (917 nm) and on the $6P_{3/2}$–$6D_{3/2}$ line (921 nm) as a function of the nanocell thickness L. These preliminary data, recorded with a YAG nanocell, have not been corrected for possible shifts induced by the strong atomic density (T = 300°C) or by the strong pump intensity populating Cs($6P_{3/2}$), and do not take into account the shape asymmetry attached to the vW interaction. In any case, the basic trend of L^{-3} behavior (continuous fitting lines) is clearly visible with a shift following CL^{-3}, where $C \sim -440$ kHz μm^3 for the 917-nm line and $C \sim -300$ kHz μm^3 for the 921-nm line. This is in spite of the limited frequency resolution of the laser (~500 MHz).

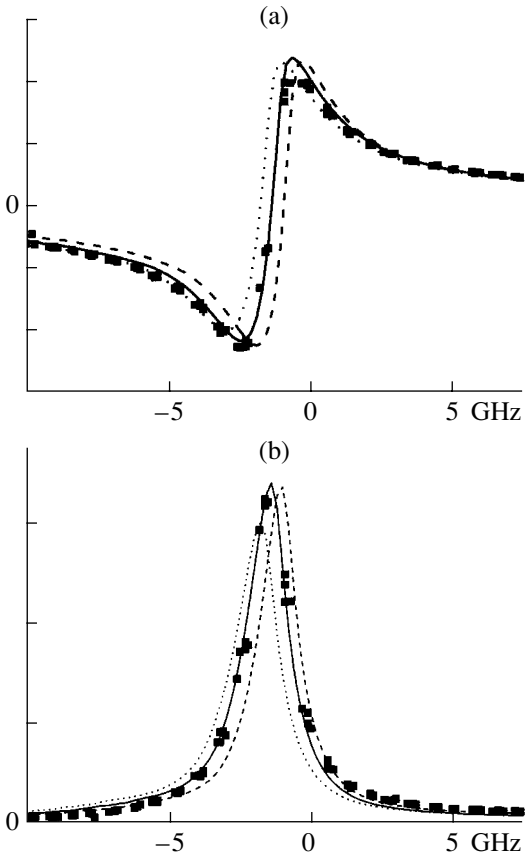

Fig. 6. Experimental reflection (a) and transmission (b) spectra as recorded on the Cs $6P_{3/2}$–$6D_{5/2}$ line (917 nm) for a 65-nm cell thickness with YAG windows, along with examples of fits that include the vW interaction. The pressure shift is experimentally confirmed to be negligible. The fits are insensitive to the fitting width (here taken to be 200 MHz), and the model assumes that the D_2 line pumping induces a "thermal" population in the $6P_{3/2}$ level (the quality of the fitting has been improved by taking a relatively small temperature of 200K). The full line assumes an interaction of 9 kHz μm^3 vW (for a single wall); the dotted line, 12 kHz μm^3; and the dashed line, 6 kHz μm^3. The horizontal scale indicates the laser frequency detuning (with a ~100-MHz accuracy) relatively to the free-space resonance.

component of the Cs 6*P*–6*D* transition [3], to extend the modeling used previously for a resonance transition to transitions between excited states, taking into account a much stronger vW interaction. On this basis, it is possible to extract an acceptable range of vW strengths from each individual spectrum, recorded for various temperatures (i.e., atomic densities), and to check the consistency of the extracted widths with a pressure broadening and eventual pressure-induced shift (with the vW shift and its induced inhomogenous broadening being clearly dominant, at least for small-thickness experiments, the pressure shift can most often be assumed to be negligible). In major contrast to SR spectroscopy, the shift of the peak position as recorded with nanocell spectra seems to impose strict limits on the range of acceptable vW strengths, while the uncertainty affecting the transition width remains much larger (conversely, in SR spectroscopy, it is often relatively easy to extract an optical width, with a large remaining uncertainty for the vW strength [3]). In addition, the experiments with nanocells permit the simultaneous recording of the transmission and reflection line shapes; hence, they provide complementary information with no need for extra fitting parameters. This obviously imposes tight constraints to the acceptable fits. Very preliminary fits have already been obtained for experiments performed at 65 nm (see Fig. 6), which provides an encouraging test of the validity of the model. It has also been experimentally noted that, in spite of strong differences in the reflection and transmission line shapes, the "apparent" shifts (as defined by the peak values in transmission or by the zeros in reflection) appear to be nearly equal for transmission and reflection line shapes, although they result [5] from a very different combination of absorption-related and dispersion-related line shapes.

Let us also mention that, in the course of these systematic experiments with nanocells, it appears to be a crucial requirement to test the reproducibility of the recorded spectra, notably because any impurity and/or charge sticking onto the windows is liable to induce dramatic effects on the atomic energy levels. For our present experiments, performed on a nanocell with

YAG windows, line-shape reproducibility has been clearly verified when comparing different cell spots of equal thickness, as long as this thickness is 65 nm or more. The comparison of 50-nm spots shows some variations in the line shapes, although several spots appear able to provide nearly identical responses that are then selected as the valid response for 50 nm (see Fig. 4). For different 40-nm spots, no effective reproducibility has been found. Rather, the apparent shift relative to the free-atom resonance varies from spot to spot by a factor that remains smaller than two in all cases. In spite of the accuracy of the thickness measurement, which apparently reaches 1–2 nm in some cases, the measurement intrinsically provides a thickness *averaged* over the optical spot size (a typical beam diameter is 100–200 μm). Hence, the nonmeasured local irregularities affecting the window profiles (i.e., roughness over various characteristic lengths) induce local fluctuations in the atom–surface distance and are expected to produce dramatic effects on the averaged atomic spectra, especially for smaller distances, with respect to a potential essentially sensitive to the *inverse cube* of the distance.

3. RESONANT ATOM–DIELECTRIC COUPLING IN NANOCELLS

The theoretical model mentioned in Section 2 relies on an electrostatic description of the vW interaction and uses a multiple-image approach to take into account the two neighboring interacting surfaces. Such a vW description, which leads to an overall spatial dependence of the vW interaction that follows a special function (the transcendental Lerch function [14]), is obviously more precise than the simple addition of the individual potential exerted by each of the walls, even if the overall spectral predictions are most often not very different.

This electrostatic approach applies only as long as the resonant couplings between the dielectric surface and the relevant virtual atomic transitions are not considered. Indeed, the vW atom–surface interaction is a dipole–dipole interaction that originates from the coupling between the atomic dipole fluctuations (to be expanded along the virtual electric dipole transitions) and the correlated fluctuations induced in the surface. Resonances in the electromagnetic coupling between a surface polariton mode and an atom fluctuation (in virtual emission) have been shown to lead to giant and possibly repulsive interaction [3, 15], along with an increased decay rate from the considered excited state [16], as governed by a surface response $(\varepsilon - 1)/(\varepsilon + 1)$, where ε is the *complex* dielectric permittivity. In particular, the 12.15-μm virtual emission of Cs($6D_{3/2}$) towards ($7P_{1/2}$) makes a sapphire surface strongly repulsive for a Cs($6D_{3/2}$) level, while a YAG surface is expected to exert only a weak repulsion [3, 17].[1] Conversely, the Cs($6D_{5/2}$) level, with its main virtual emission at 14.6 μm, is expected to remain attracted by a surface such as sapphire or YAG. This predicted difference between the two fine-structure components of the Cs(6*D*) level could not be investigated before in SR spectroscopy due to a lack of adequate sources. With the broad tuneability of our 917–921-nm source, one may naively expect to uncover these predicted differences in our present nanocell spectroscopy experiments. Actually, the situation appears to be very different for a nanocell due to its two coupled neighboring walls.

Until now, our experiments performed at small thickness of a YAG nanocell have shown no sensitive differences between the two fine-structure components, only a smaller amplitude (even when compared to the theoretical free-space ratio) for the 921-nm line ($6D_{3/2}$) and a width about twice as large (Fig. 4). In particular, no simple repulsive behavior seems to be observed for the Cs($6D_{3/2}$). In light of recent theoretical developments [18], this does not appear very much as a surprise. Indeed, in a nanocell, the surface resonances that would be responsible for a possible enhancement of the atom–surface interaction in a half free space, actually couple and shift via evanescent mode overlapping. Hence, the fluctuating atomic dipole interacts with all the modes, symmetric and antisymmetric [19], of a waveguide that appear in an electrostatic description. A major result (Fig. 7) is that, for a given atomic virtual transition, resonant coupling with the waveguide can lead to opposite behaviors between a position close to one of the walls (e.g., a red shift), and a more central position (e.g., a blue shift appears where an attractive potential is minimal). This behavior can anyhow be predicted from the resonant behavior of a single wall in the limit where the atom is close to one of the walls. Note that for a nanocell, the waveguide thickness remains very small relative to the IR wavelengths of the interacting atom, so that the electromagnetic field mode structure is modified, implying modifications for the dispersive response of the atom–dielectric coupling. Besides, if the atom under consideration is prepared in a special manner (e.g., Zeeman polarized), one may become able to discriminate between the respective fluctuations of the parallel and perpendicular atom dipoles, which are predicted to exhibit different and even opposite (repulsion vs. attraction) behaviors. More generally, it is an interesting issue, one whose solution is in progress, to know to what extent the resonant coupling of an atom located between two close surfaces will resemble the potential for the same atom embedded in the bulk of a similar material

4. ATOMIC COLLISIONS UNDER CONFINEMENT

Spectroscopy close to an interface, notably SR spectroscopy, has been for a long time a choice method to evaluate collisional broadening and shift in an optically

[1] This prediction that we have finally verified in [3], is actually dependent on the YAG description, see [17].

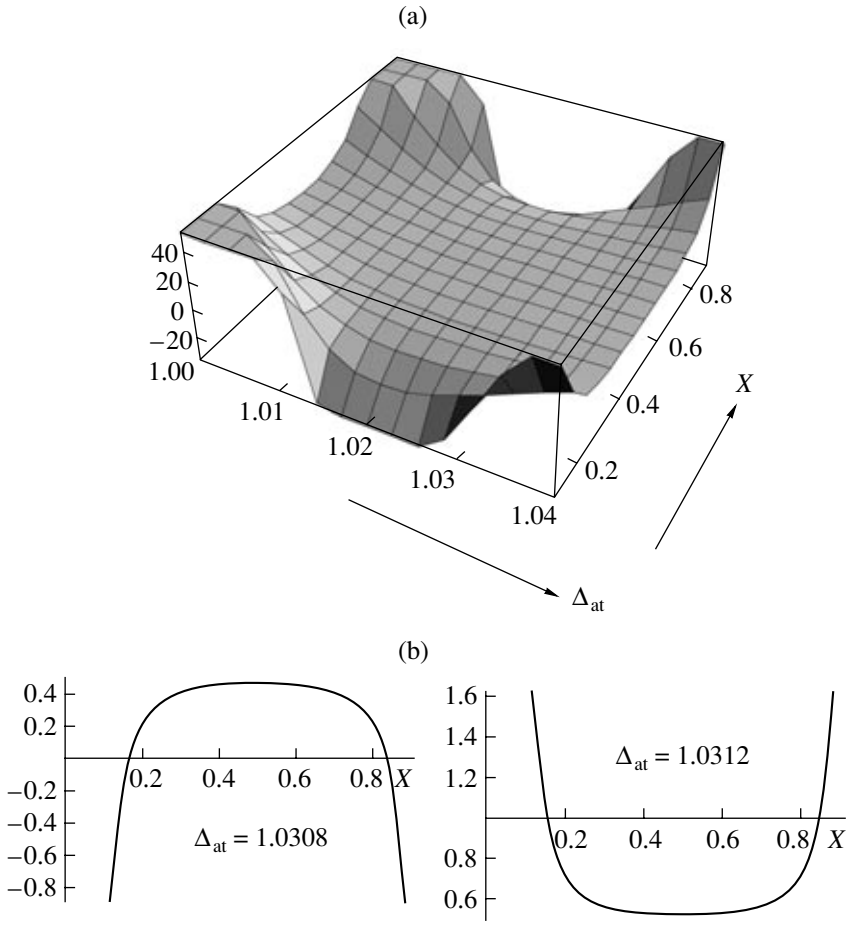

Fig. 7. Resonant contribution to the potential exerted onto an atom located between two walls (at the relative distance $x = z/L$). Calculations are for the parallel dipole contribution. In (a), a 3D representation of the potential curves (vertically truncated) is provided as a function of the relative frequency Δ_{at} ($\Delta_{at} = \omega_{at}/\omega_s$) of the virtual atomic transition (assumed to be a single one at ω_{at}) relative to the surface resonance ω_s. This dispersive resonance (whose relative width is here assumed to be 0.04) implies an atomic energy shift for a single wall that goes from positive to negative values when the relative atomic frequency Δ_{at} ($\Delta_{at} = \omega_{at}/\omega_s$) goes across the surface resonance ($\Delta_{at} = 1$). In (b), the potential curves appear to be surface-attractive ($\Delta_{at} = 1.0308$) or surface-repulsive ($\Delta_{at} = 1.0312$) irrespective of the sign of the energy shift (i.e., the attraction here is compatible with a positive shift at the center for $\Delta_{at} = 1.0308$).

dense gas. A notable advantage of these methods is that the information is obtained close to the resonance line center [20], not in the far spectral wings, as is the case with standard volume experiments. However, the implicit assumption is that the vicinity of the surface has not modified the collisional features themselves. This means, on the one hand, that the atom dynamics—i.e., the velocity distribution and the population distribution—is assumed to be identical in the gas bulk and close to the surface and, on the other hand, that the intrinsic mechanism of interaction between an atom and its perturber remains unaffected. For these reasons, we have started to investigate the collisional effects in nanocell spectroscopy for the relatively elementary case of a resonant transition.

For given conditions in a nanocell, the overall pressure broadening and shift can be extracted once the Fabry–Perot effects and surface interaction have been analyzed. Assuming that the local vapor density is the same whatever the local thickness may be, it also becomes possible to analyze the significance of eventual differences appearing for various cell thicknesses. Moreover, if it is assumed that the equilibrium atomic density is the same in a nanocell and in a macroscopic vapor, varying the nanocell temperature should yield the pressure dependence (broadening and shift) of the resonances, which are usually expected to be linear in a large density regime. Alternately, the amplitude of the spectroscopic signal itself is a valid indicator of the number of active atoms, yielding complementary data on the "vapor" equilibrium inside the nanocell.

Until now, our detailed experiments, performed on the well-resolved Cs D_1 line, have been limited to the comparison of a $\lambda/2$ and $\lambda/4$ thickness, while systematic experiments for a shorter thickness, including a variation of the temperature, are planned for the near

future. The frequency resolution allowed by such cell thicknesses is sufficient to discriminate the pressure behavior of the individual hyperfine components—exhibiting considerable differences as far as the pressure-induced shift is concerned—and should enable a comparison with independent measurements through SR spectroscopy [21].[2] Recently, a custom cell was fabricated that, designed for the simultaneous recording of a SR signal and of a transmission signal in nanometric regions, should ensure similar experimental conditions for these two spectra, with no need for a comparison involving relatively inaccurate temperature measurements. As shown in Section 2, preliminary theoretical fittings seem slightly improved when the vW interaction is included for the λ/4 thickness (the difference is not observable for a λ/2 cell). Remarkably, and although the extrapolated pressure shift is strongly modified when taking into account the vW shift, there appears (see Fig. 8) a persistant difference in the pressure shifts for a λ/2 and λ/4 thickness, which is more important than the slight difference occurring in the pressure broadening once the vW interaction is taken into account. The actual strength of the vW interaction is not only derived from the optimization of the fitting spectra but also from its ability to cancel the residual shift at null pressure, between the extrapolated resonances in the nanocell and in a macroscopic cell. However, more precise investigations are needed, because the widths become identical for λ/2 and λ/4 when the (tiny) vW interaction is neglected in the fitting process, and because of the limited number of pressure conditions that were explored for λ/4. Indeed, including a vW interaction in the fitting model shifts the estimated resonance center at the expense of a correlated modification of the evaluated optical width. Hence, the significance of the observed small apparent shift between the extrapolated frequency at zero pressure and the free-space resonance should be confirmed before ascertaining evidence of a different pressure behavior for λ/2 and λ/4 cells.

This possibility of a thickness-dependent collisional behavior is worth discussing from a general point of view. An atom–atom collision, in principle, is not very different from an atom–surface collision, especially at a long distance. In particular, the atom–atom vW interaction is nothing more than the dipole–dipole coupling between the fluctuating atomic dipole and the correlated induced (fluctuating) dipole in the atomic perturber. As long as an electromagnetic boundary lies in the vicinity of the two interacting atoms, the correlation between the fluctuations seen by the atom and its perturber can follow a variety of paths, from direct propagation to paths involving reflection(s) on the boundary [22]. Physically, these additional contributions can be understood as being equivalent to a collision process in which at least one of the atoms is replaced by its electric image. In principle, these contributions have to be considered when the distance to the reflecting plane remains smaller than the wavelength of the relevant (virtual) atomic transitions. To our knowledge, no evaluation of this confinement effect has ever been performed with the required averaging over atomic positions and velocities in the case of a confined vapor. In any case, in spite of the fact that these additional terms always exist for a nanocell (the distance to the surface being much smaller than the wavelength of the relevant virtual transitions), the dominant contribution to atom–

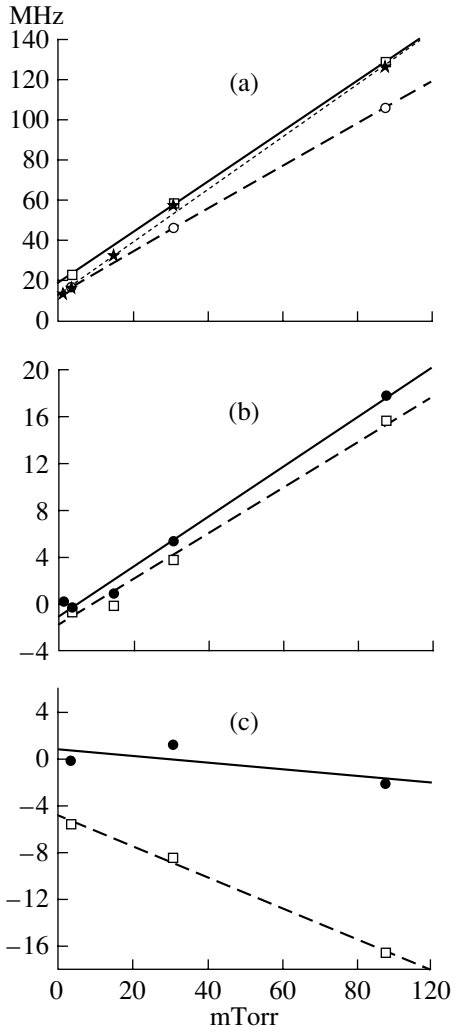

Fig. 8. Width (a) and shift (b, c) as a function of the Cs pressure as obtained from a fitting of the transmission line shapes for the $F = 4 \longrightarrow F' = 4$ component of the D_1 line. In (a), the open squares are for a λ/2 thickness (identical widths with and without van der Waals); the open circles and stars are for a λ/4 thickness with and without the vW interaction taken into account, respectively; in (b) and (c), respectively standing for a λ/2 and a λ/4 cell thickness, the closed circles are for a model with the vW interaction taken into account, while the open squares are for a model neglecting the vW interaction. The vW interaction strength is taken to be 1.8 kHz μm^3 for a single wall.

[2] See also preliminary results for Cs D_1 line in G. Dutier, *Doctoral Dissertation* (Université Paris13 (2003), unpublished).

atom collisions is expected to appear only at much shorter distances, which are related to the interatomic interaction potential (scaling as r^{-6} or r^{-3} for a resonant collision, where r is the interatomic distance). This would imply that the confinement effect should appear only at distances much smaller than a wavelength that is comparable to the one associated with the (square root of the) collision cross section, namely, on the order of 10^{-1} cm^2 for a resonant collision, a distance that remains within the reach of nanocell technology.

5. CONCLUSION

It is amazing to see how high-resolution techniques employed both in experiments and in theoretical interpretations are still applicable to uncooled atoms at such small distances from a macroscopic object. Also remarkable is the fact that, in spite of a strong 1D confinement, the vapor behaves inside the nanocell according to the behavior expected for a macroscopic vapor. Extensions of our investigations to the physics of resonant gases under strong multidimensional confinement, which can be approached with systems such as perforated fibers or porous media [23], should offer renewed surprises of interest for both fundamental and applied physics.

ACKNOWLEDGMENTS

This work has been partially supported by European contract HPRN-CT-2002-00304 as part of the FAST-Net program. We also acknowledge the French–Uruguayan ECOS program (U00-E03) and the specific support of CNRS for French–Armenian cooperation (project 12856) and of Université Paris 13 for scientific cooperation with Russia and the C.I.S. Y. Li was supported by a grant of Chinese Academy of Sciences.

REFERENCES

1. S. Briaudeau, D. Bloch, and M. Ducloy, Phys. Rev. A **59**, 3729 (1999); S. Briaudeau, S. Saltiel, G. Nienhuis, *et al.*, Phys. Rev, A **57**, R3169 (1998); S. Briaudeau *et al.*, J. Phys. IV **10**, 145 (2000); S. Briaudeau *et al.*, *Laser Spectroscopy: XIII International Conference, Hangzhou, China, 1997*, Eds. by Y. Z. Wang, *et al.*, (World Scientific, Singapore, 1998), pp. 33-36.
2. D. Bloch and M. Ducloy, "Atom-Wall Interaction", Adv. At. Molec. Opt. Phys. **50**, 91–154 (2005); Eds. by B. Bederson and H. Walther (Academic, San Diego, 2005) (in press).
3. H. Failache, S. Saltiel, M. Fichet, *et al.*, Phys. Rev. Lett. **83**, 5467 (1999); Eur. Phys. J. D **23**, 237 (2003).
4. D. Sarkisyan, D. Bloch, A. Papoyan, and M. Ducloy, Opt. Commun. **200**, 201 (2001).
5. G. Dutier, S. Saltiel, D. Bloch, and M. Ducloy, J. Opt. Soc. Am. B **20**, 793 (2003).
6. G. Dutier, A. Yarovitski, S. Saltiel, *et al.*, Europhys. Lett. **63**, 35 (2003).
7. R. H. Romer and R. H. Dicke, Phys. Rev. **99**, 532 (1955).
8. D. Sarkisyan, T. Varzhapetyan, A. Sarkisyan, *et al.*, Phys. Rev. A **69**, 065802 (2004).
9. R. H. Dicke, Phys. Rev. **89**, 472 (1953); Phys. Rev. **96**, 530 (1954).
10. T. Varzhapetyan, D. Sarkisyan, L. Petrov, *et al.*, in *Proceedings of the XIII International School on Quantum Electronics "Laser Physics and Applications," SPIE, Burgas, Bulgaria, 2004* (Burgas, Bulgaria, 2004); D. Sarkisyan, T. Varzhapetyan, A. Papoyan, *et al.*, "Absorption and Fluorescence in Atomic Submicron Cell: High Laser Intensity Case," in *Proceedings of International Conference on Coherent and Nonlinear Optics (ICONO), St. Petersburg, Russia, 2005* (in press).
11. S. Briaudeau, D. Bloch and M. Ducloy, Europhys. Lett. **35**, 337 (1996); A. Ch. Izmailov, Laser Phys. **2**, 762 (1992); Opt. Spectrosk. **74**, 41 (1993) [Opt. Spectrosc. **74**, 25 (1993)].
12. V. Sandoghdar, C. I. Sukenik, E. A. Hinds and S. Haroche, Phys. Rev. Lett. **68**, 3432 (1992); V. Sandoghdar, C. I. Sukenik, S. Haroche and E. A. Hinds, Phys. Rev. A **53**, 1919 (1996).
13. G. Dutier, I. Hamdi, P. C. S. Segundo, *et al.*, in *Proceedings of the XVI International Conference on Laser Spectroscopy*, Eds. by P. Hannaford, A. Sidorov, H. Bachor, and K. Baldwin (World Scientific, Singapore, 2004), pp. 277–284.
14. H. Nha and W. Jhe, Phys. Rev. A **54**, 3505 (1996); and erratum **60**, 1729 (1999).
15. M. Fichet, F. Schuller, D. Bloch, and M. Ducloy, Phys. Rev. A **51**, 1553 (1995); M. Wylie and J. E. Sipe, Phys. Rev. A **30**, 1185 (1984); Phys. Rev. A **32**, 2030 (1985).
16. H. Failache, S. Saltiel, A. Fischer, *et al.*, Phys. Rev. Lett. **88**, 243603 (2002).
17. *Handbook of Optical Constants of Solids*, Ed. by E. D. Palik (Academic Press, San Diego, 1998), Vol. 3; S. Saltiel *et al.* (in preparation).
18. M.-P. Gorza (in preparation).
19. C. Henkel, K. Joulain, J.-Ph. Mulet, and J.-J. Greffet, Phys. Rev. A **69**, 023808 (2004).
20. A. M. Akul'shin, V. L. Velichanskii, A. S. Zibrov, *et al.*, Zh. Eksp. Teor. Fiz. **36**, 303 (1982) [Sov. Phys. JETP **36** (7), 247 (1982)].
21. N. Papageorgiou, M. Fichet, V. A. Sautenkov, D. Bloch, and M. Ducloy, Laser. Phys. **4**, 392 (1994).
22. M. Cho and R. J. Silbey, J. Chem. Phys. **104**, 8730 (1996).
23. A. Burchianti, C. Marinelli, A. Bogi, *et al.*, Europhys. Lett. **67**, 983 (2004).